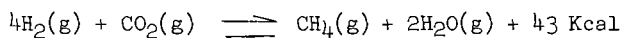KINETICS OF CARBON DIOXIDE METHANATION ON
A RUTHENIUM CATALYST

Peter J. Lunde and Frank L. Kester

Hamilton Standard Division,
United Aircraft Corporation
Windsor Locks, Connecticut, 06096

INTRODUCTION

The catalytic hydrogenation of carbon dioxide to methane

$$4H_2(g) + CO_2(g) \rightleftharpoons CH_4(g) + 2H_2O(g) + 43 \text{ Kcal}$$

is often called the Sabatier reaction, after the Belgian chemist who investigated the hydrogenation of hydrocarbons using a nickel catalyst. The Sabatier reaction is becoming of commercial interest for the manufacture of natural gas from the products of coal gasification. The reverse reaction, of course, is called steam reformation and is a commercial method for hydrogen manufacture.

This paper developed from work performed under contract to NASA to investigate the Sabatier reaction as a step in reclaiming oxygen within closed cycle life support systems. Carbon dioxide from the cabin atmosphere is thus changed into water vapor which is electrolyzed to provide oxygen for the cabin plus one-half the hydrogen required for the Sabatier reaction. The rest of the hydrogen is provided from the electrolysis of stored water, which produces breathing oxygen as a by-product, reducing the proportion of available carbon dioxide which must be reacted and assuring excess carbon dioxide in the feed mixture.

The Sabatier reaction is a reversible, highly exothermic reaction which proceeds at a useful rate at the low temperatures required for high yields only when a catalyst is used. Dew, White, and Sliepcevitch (1) studied this reaction using a nickel catalyst. This paper examines the kinetics of the reaction using a Ruthenium catalyst, and derives from experimental data a correlation describing the kinetics of this catalysis in the $400°F$ to $700°F$ temperature range.

Thermodynamics

Equilibrium compositions for hydrogen and carbon dioxide mixtures at 1 atm are shown in Figure 1, which was prepared with the aid of a computer program developed by United Aircraft Research Laboratories using free energies from Wagman (2). Carbon and carbon monoxide are possible products, as well as methane and water vapor. The reaction proceeds as written

$$4H_2(g) + CO_2(g) \rightleftharpoons 2H_2O(g) + CH_4(g)$$
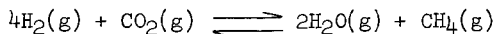
for molar feed ratios ($H_2:CO_2$) of over 3.5:1 at temperatures from $400°F$ to $700°F$.

Low temperatures favor high conversions. At $700°F$ and a feed ratio ($H_2:CO_2$) of 3.5:1 the equilibrium conversion of H_2 is only 90%, while at $400°F$ it is about 99%.

As the feed ratio falls below 3.5:1, carbon becomes thermodynamically stable at higher and higher temperatures. At 3:1, carbon deposition is possible only below $500^{\circ}F$ while at 2:1 it is stable below $1100^{\circ}F$.

Carbon monoxide formation is thermodynamically possible above $700^{\circ}F$, where the reaction encounters the well-known "water gas shift".

$$CO_2 + H_2 \rightleftharpoons CO + H_2O$$
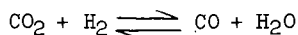
This does not cause a limitation in maximum operating temperature because any carbon monoxide formed is converted to other products downstream in the reactor's subsequent $400^{\circ}F$ - $700^{\circ}F$ temperature zone which is necessary for a practical yield.

<div align="center">EXPERIMENTAL</div>

Catalyst Selection

Thompson (3) conducted a Sabatier catalyst screening program for the US Air Force. Four catalysts were experimentally evaluated:

1) Nickel (80% Ni and NiO) on kieselguhr)
2) 0.5% ruthenium (on alumina)
3) 0.5% rhodium (on alumina)
4) 0.5% cobalt (on alumina)

Ruthenium and nickel were found to be appreciably more active catalysts for promoting the Sabatier reaction. Nickel, however, presented several operating problems.

1) Slow deterioration over the test period, attributed to sulfur poisoning.
2) Reactor startup in hydrogen was advisable to assure reduction of nickel to its most active form.
3) Carbon deposition was reported at $650^{\circ}F$ to $700^{\circ}F$.

Ruthenium had none of these problems, and was somewhat more active than the nickel as a catalyst. Furthermore, there was a potential for even more activity if heavier loadings of the metal on the substrate are used.

Consequently a 0.5% ruthenium catalyst on 1/8 in x 1/8 cylindrical alumina pellets was selected for further investigation. The prepared catalyst, Englehard type "E", was purchased from

Englehard Industries Division
Englehard Minerals and Chemicals Corp.
113 Aster Street
Newark, N. J.

The manufacturer furnished no lot number or other specific information but did disclose that the catalyst performed within the limits of their internal specifications. Superficial examination of the pellets indicated the ruthenium did not penetrate more than 1/2 mm into the alumina indicating that pore diffusion was not likely to be important in the performance of this catalyst. The bulk density of the pellets was measured as 1.0 g/cc.

Approach

The ruthenium catalyst is relatively new and there are no published quanti-
tative data from which the kinetics can be determined. Consequently, an experi-
mental apparatus was designed and a program to acquire rate data was begun.

Hydrogen and carbon dioxide were fed continuously to the experimental apparatus.
The test reactor, a tube filled with catalyst and held isothermal by immersion in
a molten salt bath, was made small so that the conversion of unreacted feed was low
but measurable at the lowest operating temperature, minimumizing the reaction heat
released. At higher temperatures part of the feed was passed through a large
"supply" reactor providing a partly reacted feed to the test reactor which reduced
the reaction rate and the reaction heat released.

Steady state conversions were determined from flow information and chromato-
graphic analyses of the test reactor inlet and outlet streams. Mass flow to the
reactor was held steady for runs at several temperatures, giving data for calcula-
tion of the reaction activation energy, which describes the temperature dependence
of the reaction rate. Additional runs were made at constant temperature to deter-
mine the basic reaction rate constant.

Feed flow ratios ($H_2:CO_2$) of 2:1 and nearly 4:1 were investigated. Tempera-
tures of $400^\circ F$ to $700^\circ F$ were selected for activation energy data accumulation
since at temperatures over $700^\circ F$ the reaction proceeds rapidly and is complicated
by carbon dioxide formation, while $400^\circ F$ is low enough to allow virtually complete
conversion of the feed in a practical reactor.

Apparatus

A schematic for the complete experimental rate data apparatus is shown in
Figure 2.

The feed rates of hydrogen and carbon dioxide were set externally using
laminar flowmeters. Electronic differential pressure sensors converted a differen-
tial pressure flow signal to an electrical voltage which was read on a digital
voltmeter. The flowmeter calibrations are shown in Figure 3.

When desired, partially reacted feed was produced by passing part of the mixed
feed flow through a "supply" Sabatier reactor. This reactor, which also used a
ruthenium catalyst, was heated to about $650^\circ F$ and was large enough to react 80% -
90% of the stoichiometrically lean feed constituent.

Sampling

All samples except the inlet feed were fed to a Bendix process chromatograph
at very low flow (Figure 2, S1, S2, S4, S5). The inlet feed sample (S3) was taken
by actuating two three-way valves which directed the entire feed stream through the
chromatograph sampling valve. A sample could be taken in this manner without
changing the feed flow rate. When other samples were being taken the pressure drop
of the chromatograph sampling valve (about 0.6 - 0.8 psi) was simulated in the
feed line with a precision metering valve (marked "ADJ") set to maintain a constant
pressure at PI-2 so that there was no transient when the feed sample valves were
actuated. Heating tape and heated valve boxes were necessary throughout the sampl-
ing system to prevent water from condensing in the sample lines.

The process gas chromatograph analyzed feed and effluent gases using samples
of equal volume for analysis. Peaks were automatically gated, attenuated and

recorded. Peak heights were then manually measured and logged as raw composition data. Components analyzed were H_2O, CO_2, H_2, CO, CH_4, N_2, Ar, and O_2, but the last three were not present in significant quantities. A typical chromatogram is shown in Figure 4. Each analysis took 13 minutes and was always repeated before data was recorded.

The chromatograph was calibrated by using pure CO_2, H_2, and CH_4, at several pressures in the 0-1 atm range. The chromatographic peak heights then corresponded to partial pressures of the calibrated constituents. Water was calibrated indirectly using Sabatier reactor effluent, in which the partial pressure of water vapor was necessarily exactly twice that of the methane which was already calibrated. Final calibration curves for the chromatograph are shown in Figure 5.

After the chromatograph was calibrated, the hydrogen peak signal became erratic during the data collection phase. Successful gas analyses were continued by taking the correct hydrogen partial pressure as equal to the difference between analysis pressure and the sum of the other constituents as determined from their peak heights and calibration curves. The accuracy of this method was confirmed later in this work after the electronic malfunction responsible was repaired.

Test Reactor

The differential reactor used for the actual kinetic study was made from 1/2 in. stainless steel tubing (0.43 in ID x 1.75 in). The catalyst charge of 3.58 grams (about eighty 1/8 in. x 1/8 in. cylindrical alumina pellets coated with 1/2% ruthenium) filled the 4.15 cc reactor tube. The reactor was called the "differential" reactor because its purpose was to convert only a small portion of the feed stream to the Sabatier products.

The differential reactor assembly, consisting of a feed preheating coil, thermocouples and sample tubes (Figure 6) was submerged in an oven-heated molten salt bath to keep the reactor isothermal, because of the high heat of reaction. Thermocouples were installed in the inlet stream (T2), outlet stream (T4), at the center of the reactor (T3), and on the reactor wall (T5). Samples could be taken from the feed (after preheat) (S4), effluent (S5), and (externally) from the feed before entering the reactor.

At the low end of the temperature range (400° - 500°F) reaction rates were low and the reactor wall and center thermocouples agreed $\pm$ 1°F. At higher temperatures the reaction rate was high and the reaction rate was reduced so that the temperature differential was held below 10°F by partly reacting the inlet feed before it entered the differential reactor. Using this technique good experimental data could be taken from 400°F to 700°F in a single reactor with a constant feed rate.

<div align="center">DISCUSSION</div>

Since the mechanism for ruthenium catalysis is unknown, gas phase type kinetics are proposed for the reaction:

$$4H_2(g) + CO_2(g) \underset{kr}{\overset{kf}{\rightleftharpoons}} 2H_2O(g) + CH_4(g)$$
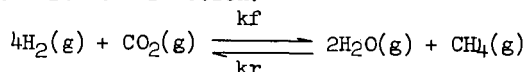
where k_f and k_r represent reaction rate constants for the forward and reverse reactions, respectively. Thus

$$- \frac{d\left[P_{CO_2}\right]}{dt} = k_r^n \left[P_{H_2O}\right]^{2n} \left[P_{CH_4}\right]^n - k_f^n \left[P_{CO_2}\right]^n \left[P_{H_2}\right]^{4n} \tag{1}$$

where n is an emperical constant equal to 1 for pure gas phase kinetics.

When equilibrium is achieved, $-d\left[P_{CO_2}\right]/dt = 0$, and equation (1) becomes

$$K_e = \frac{k_f}{k_r} = \frac{\left[P_{H_2O}\right]^2\left[P_{CH_4}\right]}{\left[P_{CO_2}\right]\left[P_{H_2}\right]^4} \tag{2}$$

and the emperical exponent applied to the exponential coefficients cancels so that the equilibrium constant, K_e, is defined as a classical thermodynamics.

Noting the $K_e^n = k_f^n/k_r^n$, if equation (1) is rewritten $\qquad$ (3)

$$-\frac{d\left[P_{CO_2}\right]}{dt} = k_f^n \left\{ \left[P_{CO_2}\right]^n\left[P_{H_2}\right]^{4n} - \frac{\left[P_{CH_4}\right]^n\left[P_{H_2O}\right]^{2n}}{(Keq(T))^n} \right\} \tag{4}$$

then the temperature dependence of the reaction rate constants can be described by the general Arrhenius relationship

$$k_f^n(T) = k \exp(-E_a/RT) \tag{5}$$

and thus the final form of the rate expression is

$$-\frac{d\left[P_{CO_2}\right]}{dt} = k \exp(-E_a/RT) \left\{ \left[P_{CO_2}\right]^n\left[P_{H_2}\right]^{4n} - \frac{\left[P_{CH_4}\right]^n\left[P_{H_2O}\right]^{2n}}{(Keq(T))^n} \right\} \tag{6}$$

where k (the rate constant) and Ea (the activation energy) and n (catalyst coefficient) are constants to be determined for the experimental data.

To find the activation energy E_a and catalyst coefficient n for equation (6) the logarithms of both sides are taken. Rearrangement then gives

$$Y \equiv \ln \frac{-d\left[P_{CO_2}\right]/dt}{\left[P_{CO_2}\right]^n\left[P_{H_2}\right]^{4n} - \frac{1}{K_{eq}^n}\left[P_{CH_4}\right]^n\left[P_{H_2O}\right]^{2n}} = \left[\frac{E_a}{R}\right]\left[\frac{1}{T}\right] + \ln k \tag{7}$$

which is of the form Y = mX + b. A plot of Y vs 1/T thus has a slope of Ea/R, enabling determination of Ea. The catalyst coefficient n can be determined by trial because improper values of n do not give a linear plot of experimental data.

With Ea and n determined, equation (6) can be now integrated to obtain a value of rate constant k for each experimental run.

Rearranging and solving equation (6) for k

$$k = e^{-Ea/RT} \left[\frac{dP_{CO_2}}{dt}\right] \left[\frac{-1}{\left[P_{CO_2}\right]^n\left[P_{H_2}\right]^{4n} - \frac{1}{K_{eq}^n}\left[P_{CH_4}\right]^n\left[P_{H_2O}\right]^{2n}}\right] . \tag{8}$$

If the change in P_{CO_2} as it passes through the reactor is defined as X, then the variables can be separated

$$k = e^{-Ea/RT} \frac{dX}{dt} \left[\frac{-1}{\left[P_{CO_2}^{in} - X \right]^n \left[P_{H_2}^{in} - 4X \right]^{4n} - \frac{1}{K_{eq}^n} \left[X \right]^n \left[2X \right]^{2n}} \right] \quad (9)$$

where $P_{CO_2}^{in}$ and $P_{H_2}^{in}$ are inlet partial pressures.

Integrating equation (9) from reactor inlet to outlet,

$$k = e^{-Ea/RT} \frac{\displaystyle\int_{0}^{P_{CO_2}^{in}-P_{CO_2}^{out}} \frac{dX}{\left[P_{CO_2}^{in} - X \right]^n \left[P_{H_2}^{in} - 4X \right]^{4n} - \frac{1}{K_{eq}^n} \left[X \right]^n \left[2X \right]^{2n}}}{\displaystyle\int_{t_{in}}^{t_{out}} dt} \quad (10)$$

Since space velocity $S_v = \frac{1}{t}$ where t is contact time,

$$k = e^{-Ea/RT} S_v \int_{0}^{P_{CO_2}^{in} - P_{CO_2}^{out}} \left[\frac{dX}{\left[P_{CO_2}^{in} - X \right]^n \left[P_{H_2}^{in} - 4X \right]^{4n} - \frac{1}{K_{eq}^n} \left[X \right]^n \left[2X \right]^{2n}} \right] \quad (11)$$

The integral involves only inlet and outlet concentrations, known kinetic constants and the running variable X, and can be solved by numerical or graphical techniques. Values of $K_{eq}(T)$ were obtained from (2).

A standard fourth order Runge-Kutta numerical integration technique was carried out for each test run using a computer program written explicitly for this work. The Runge-Kutta method, which employs a Taylor series expansion of the derivative function, was selected because of its accuracy and stability (4).

<div align="center">RESULTS</div>

Two series of data were taken using the differential test reactor. The activation energy series was run over a wide temperature range at low reaction rates to determine activation energy and catalyst coefficient. The reaction rate series was run at a single temperature and varying reaction rates to determine the reaction rate coefficient.

Table I shows the complete experimental data after preliminary processing.[1]
Table II shows the results of activation energy calculations from equation (7)
using selected runs. Table III shows the results of integration of other selected
runs to calculate a rate constant according to equation (11). Table IV indicates
the criteria for selecting runs for these calculations.

The <u>activation energy</u> series was started at 400°F and the temperature gradually
raised to 700°F while the conversion of the inlet gas was raised from 0% to 96% to
keep the composition change across the differential reactor small (Runs 519-551).
Volumetric flow of the feed gas was held steady except for two lower value runs
at the start. The ratio of $H_2:CO_2$ in the feed gas was held just below stoichio-
metric (at 3.8) for the first temperature sweep (Runs 519-534), and at about 2.0
for the second (Runs 538.50 - 551).

The <u>reaction rate</u> series was run at bath temperatures of 580°F and 520°F and
at inlet flow ratios of 1.9 and 2.9, respectively (Runs 560-581). Inlet conver-
sions were varied from 0% to 84%. Two final runs were taken at flow ratios just
over stoichiometric (at 4.1) using lower bath temperatures providing unreacted
feed gas at 435°F and 475°F (Runs 590 and 591).

The lower inlet flow ratios of $H_2:CO_2$ in each series was within the range for
which carbon deposition was thermodynamically stable (Figure 1). No evidence for
such deposition was observed in these tests in performance degradation or after
post-test catalyst examination.

EXPERIMENTAL DATA REDUCTION

A data reduction computer program was used to produce the data presented in
Table I.

<u>Inlet and Outlet Partial Pressures</u> - Inlet analysis total pressure was taken as the
arithmetic average between supply reactor pressure (PI-2, Figure 2) and differential
reactor inlet pressure (PI-3). CO_2, H_2O, and CH_4 partial pressures were determined
from chromatographic peak heights and H_2 taken as the remaining constituent by
difference, as discussed in "Sampling", above. The partial pressures were then
normalized to total 1.000, thus becoming mol fractions, and then mutiplied by the
inlet reactor pressure (PI-3) to determine inlet partial pressures*.

The experimental outlet compositions were determined similarly, except that
the analysis pressure was taken as the arithmetic average between differential
reactor outlet (PI-4) and chromatograph outlet (PI-5). After mol fraction calcula-
tion, a new stoichiometrically exact set of outlet mol fractions was synthesized
from the inlet compositions plus the outlet CH_4 composition[2]. The synthesized
values were printed next to the experimental values for easy comparison. Generally
the values agreed within a factor of 1%, and often the agreement was much better.
Constituent outlet partial pressures* were then calculated from the synthesized
outlet composition and outlet reactor pressure.

<u>Reactor Flow Rates</u> - Laminar flowmeter voltages were converted to total volumetric
inlet flow* and then weight flow (lb/hr) using flowmeter pressure, temperature,
and the perfect gas laws. Volumetric flow rates for each constituent were then

---

[1]Complete raw data is given in Reference 5, which is the NASA report of this work.
*Presented in Table 1 for all reported test runs.
[2]This was done to avoid errors in later calculations due to experimental inaccura-
cies.

calculated at reactor inlet and outlet, taking into account the reactor temperature*, pressure, and chromatographically determined compositions while conserving only the total weight flow of the feed constituents. Contact time (sec) and space velocity* (1/hr) were calculated using the reactor volume* and average reactor flow rate. Reactor inlet and outlet flows in lb-mols/hr were then calculated, using volumetric flows and the perfect gas laws.

Reaction Rates - Molar CO_2 reaction rate (lb-mol/hr) was then calculated from the difference in inlet and outlet molar flow rates of CO_2. Then the specific conversion rate was calculated (lb-mol/hr catalyst), using catalyst weight*.

CO_2 reaction rate* in atm/hr was also calculated, using the perfect gas law at reaction conditions and the molar reaction rate.

DATA CORRELATION

Reduced run data listed in Table I was further processed to determine values of the activation energy, Ea, catalyst coefficient, n, and reaction rate coefficient, k.

Activation Energy and Catalyst Coefficient - A specail computer program was written to process reduced data from the activation energy runs to a form appropriate for graphically fitting equation (7). A least squares fit was incorporated to calculate the activation energy directly. Table II is an output from this program for n = 1/4. The data were fitted using catalyst coefficients of n = 1/4, 3/8, 1/2, and 1. When n was 1/4 or 3/8, a plot of equation (7) was generally linear (Figures 7 and 8). The data were more linear with n = 1/4 and this was selected as the catalyst coefficient, resulting in a value for activation energy of

Ea = 30,600	btu/lb mols CO_2
or		
Ea = 17.0	Kcal/g mols CO_2

Rate Coefficient - Table III is the output from the Runge-Kutta integration routine which calculates the rate constants for selected runs according to equation (11). Data for integration were selected as noted in Table IV.

The required program input for the data reduction is tabulated along with the calculated rate constant for each run. The average constant is

$$k = 2.46 \times 10^9 \ atm^{-1/4} \ hr^{-1}$$

for the constant temperature runs 544.1 to 581.0 and

$$k = 2.338 \times 10^9 \ atm^{-1/4} \ hr^{-1}$$

for the entire page of tests of Table IV.

---

*Presented in Table I for all reported test runs.

References

1. Dew, J. M., White, R. R. and Sliepcevitch, C. M. "Hydrogenation of Carbon Dioxide on a Nickel - Kieselguhr Catalyst". IEC V 47, 1, Jan. 1955 p. 140-146.

2. Wagman, D. D., et al "Heats, Free Energies, and Equilibrium Constants of Some Reactions involving O_2, H_2, H_2O, C, CO, CO_2, and CH_4". Research Paper RP 1634, J. Res. Nat. Bu. of Std., V 34, Feb. 1945, p. 143-161.

3. Thompson, Edward B. Jr. Technical Documentary Report No. FDL-TDR-64-22. "Investigations of Catalytic Reactions for CO_2 Reduction". Parts I - V, 1964 - 67. Published by:

       Air Force Flight Dynamics Laboratory
       Research and Technology Division
       Air Force Systems Command
       Wright-Patterson Air Force Base, Ohio
On sale to the general public from:
       Office of Technical Services
       Department of Commerce
       Washington, D. C.

4. Chemical Engineers' Handbook, 4th edition, John H. Perry, editor. p. 2-62 McGraw-Hill, 1963.

5. Baum, R. A., Kester, F. L. and Lunde, P. J. "Computerized Analytical Technique for Design and Analysis of a Sabatier Reactor Subsystem", Hamilton Standard report No. SVHSER 5082, (1970), prepared on NASA contract 9-9844. Available through National Technical Service Publications. Document No. 71-26295.

Table I

SUMMARY OF EXPERIMENTAL DATA AFTER PRELIMINARY PROCESSING
3.58 GRAMS CATALYST USED IN 4.15 ML REACTOR
INLET/OUTLET PARTIAL PRESSURES SUM TO INLET/OUTLET TOTAL PRESSURE
SPACE VELOCITY AND PCO2 CONSUMED CALCULATED AT REACTOR TEMP AND PRESSURE
INLET FLOW (CUBIC FT/HR) MEASURED AT 19 PSIA AND 73 DEG F
CATALYST COEFFICIENT = 0.25

TEST NUMBER	ABSCISSA X(NP) (1/DEG R)	ORDINATE Y(NP)	REACTOR TEMP. (DEG.F)	WALL TEMP (DEG F)	PCO2 CONSUMED (ATM/HR)	SPACE VELOCITY (1/HR)	INLET FLOW (CFH)	INLET CO2 (ATM)	OUTLET CO2 (ATM)	INLET H2 (ATM)	OUTLET H2 (ATM)	INLET H2U (ATM)	OUTLET H23 (ATM)	INLET CH4 (ATM)	OUTLET C44 (ATM)
519.00	0.001157	3.4184	404.	404.	16.380	1520.	0.2117	0.2036	0.2002	0.8033	0.7984	0.0	0.3115	0.0	0.0058
520.00	0.001120	4.1264	433.	433.	32.730	1548.	0.2117	0.1978	0.1911	0.8091	0.7828	0.0	0.0220	0.0	0.0110
520.10	0.00112C	4.0221	433.	433.	29.810	2877.	0.4172	0.2047	0.2015	0.8022	0.7893	0.0	0.0107	0.0	0.0054
521.00	0.00110	4.2811	443.	443.	38.510	2878.	0.4169	0.2034	0.1993	0.8035	0.7870	0.0	0.0137	0.0	0.0069
521.10	0.001069	5.1155	462.	462.	86.250	3874.	0.4172	0.1386	0.1305	0.8683	0.8427	0.0	0.0225	0.0	0.0112
521.40	0.001076	4.8554	469.	469.	67.830	3058.	0.4239	0.2036	0.1970	0.8034	0.7767	0.0	0.0222	0.0	0.0111
522.30	0.001036	5.6127	505.	505.	141.000	3021.	0.4243	0.2055	0.1899	0.8050	0.7422	0.0	0.0453	0.0	0.0226
523.30	0.001042	5.5439	500.	500.	105.500	2792.	0.4256	0.1714	0.1575	0.6814	0.6257	0.1060	0.1454	0.0517	0.0714
524.00	0.001013	5.7263	527.	52C.	127.430	2703.	0.4231	0.1790	0.1645	0.6818	0.6224	0.0987	0.1480	0.0475	0.0721
525.10	0.000986	6.2092	552.	543.	199.80C	2670.	0.4231	0.1799	0.1573	0.6826	0.5856	0.0968	0.1739	0.0476	0.0981
525.10	0.000995	6.0728	545.	537.	175.500	2671.	0.4231	0.1799	0.1600	0.680C	0.5979	0.0994	0.1575	0.0476	0.0316
526.00	0.000987	5.9528	553.	548.	115.200	2415.	0.4231	0.1487	0.1331	0.5370	0.4721	0.2141	0.2678	0.1071	0.1340
527.00	0.000965	6.3181	576.	567.	157.000	2379.	0.4231	0.1485	0.1272	0.5298	0.4409	0.2197	0.2932	0.1090	0.1457
527.10	0.000981	6.0471	559.	551.	123.500	2393.	0.4231	0.1485	0.1316	0.5298	0.4595	0.2197	0.2778	0.1090	0.1380
527.20	0.000972	6.2076	569.	560.	142.500	2385.	0.4231	0.1485	0.1291	0.5298	0.4490	0.2197	0.2865	0.1090	0.1424
528.10	0.000943	6.7065	600.	587.	218.230	2355.	0.4227	0.1477	0.1181	0.5305	0.4071	0.2197	0.3217	0.1090	0.1500
529.20	0.000945	6.7426	598.	589.	171.000	2228.	0.4223	0.1243	0.0984	0.4362	0.3280	0.2665	0.3859	0.1499	0.1946
530.00	0.000923	7.1121	623.	612.	222.830	2187.	0.4223	0.1255	0.0916	0.4299	0.2878	0.3004	0.4178	0.1510	0.2097
531.00	0.000894	7.3570	652.	639.	252.600	2166.	0.4223	0.1229	0.0846	0.4202	0.2558	0.3059	0.4380	0.1579	0.2245
532.00	0.000899	7.4365	652.	648.	64.010	1928.	0.4223	0.C714	0.0594	0.1805	0.1298	0.5023	0.5441	0.2526	0.2735
533.00	0.000860	7.7548	677.	670.	66.850	1927.	0.4223	0.C714	0.0592	0.1805	0.1267	0.5023	0.5450	0.2526	0.2740
534.00	0.000862	8.2982	700.	694.	73.170	1925.	0.4223	0.C714	0.0582	0.1805	0.1248	0.5023	0.5482	0.2526	0.2755
536.50	0.001163	3.4621	400.	400.	14.520	2836.	0.4352	0.3893	0.3874	0.6175	0.6076	0.0	0.0055	0.0	0.0027
539.50	0.001133	3.9847	423.	423.	26.910	2582.	0.4063	0.3414	0.3374	0.6654	0.6463	0.0	0.0139	0.0	0.0054
540.10	0.001124	4.1873	430.	430.	29.730	2567.	0.4063	0.3435	0.3393	0.6633	0.6427	0.0	0.0120	0.0	0.0060
540.20	0.001111	4.2998	440.	440.	36.660	2564.	0.4063	0.3435	0.3388	0.6633	0.6392	0.0	0.0147	0.0	0.0073
540.80	0.001094	4.5448	450.	450.	46.630	2559.	0.4063	0.3435	0.3382	0.6633	0.6340	0.0	0.0195	0.0	0.0093
541.10	0.001056	5.1762	485.	480.	86.020	2527.	0.4063	0.3455	0.3379	0.6613	0.6117	0.0	0.0336	0.0	0.0168
541.12	0.001056	5.1668	485.	486.	85.250	2528.	0.4063	0.3455	0.3380	0.6613	0.6121	0.0	0.0333	0.0	0.0166
542.00	0.001053	5.1734	490.	485.	85.980	2555.	0.4070	0.3434	0.3359	0.6634	0.6146	0.0	0.0330	0.0	0.0165
542.10	0.001036	5.5466	505.	505.	123.300	2538.	0.4070	0.3434	0.3336	0.6634	0.5945	0.0	0.0472	0.0	0.0236
543.00	0.001047	5.6149	495.	491.	55.830	2284.	0.4070	0.3305	0.3264	0.5117	0.4782	0.1051	0.1314	0.0595	0.0728
544.00	0.001029	5.5951	512.	505.	96.920	2263.	0.4070	0.3312	0.3241	0.5124	0.4507	0.1081	0.1539	0.0552	0.0781
544.10	0.001020	5.6702	520.	514.	103.900	2260.	0.4070	0.3312	0.3236	0.5124	0.4446	0.1081	0.1570	0.0552	0.0797
544.20	0.001012	6.0089	526.	521.	141.600	2243.	0.4070	0.3312	0.3208	0.5124	0.4221	0.1081	0.1752	0.0552	0.0898
544.30	0.001006	6.0740	534.	525.	150.100	2240.	0.4070	0.3312	0.3202	0.5124	0.4170	0.1081	0.1790	0.0552	0.0907
545.00	0.001021	5.6147	519.	512.	85.050	2151.	0.4070	0.3302	0.3226	0.4476	0.3872	0.1543	0.1973	0.0782	0.0997
545.10	0.001012	5.7134	528.	519.	93.110	2153.	0.4073	0.3302	0.3220	0.4476	0.3822	0.1543	0.2010	0.0782	0.1016
545.30	0.001006	5.6705	534.	524.	107.420	2141.	0.4070	0.3302	0.3209	0.4476	0.3722	0.1543	0.2085	0.0782	0.1053
546.10	0.000999	6.0206	541.	532.	121.530	2145.	0.4078	0.3276	0.3192	0.4427	0.3593	0.1547	0.2226	0.0779	0.1288
547.10	0.000969	6.5732	572.	558.	194.800	2106.	0.4070	0.3275	0.3125	0.4428	0.3066	0.1583	0.2578	0.0783	0.1280
548.00	0.000960	6.0161	560.	559.	56.320	1884.	0.4070	0.2647	0.2581	0.1527	0.1021	0.3941	0.4320	0.2020	0.2215
549.00	0.000955	6.9452	587.	581.	69.570	1879.	0.4070	0.2647	0.2568	0.1526	0.0914	0.3941	0.4470	0.2024	0.2755
549.10	0.000958	6.9998	590.	581.	133.500	1929.	0.4070	0.2865	0.2729	0.2477	0.1379	0.3164	0.3984	0.1632	0.2745
550.00	0.000929	7.3386	616.	604.	167.500	1922.	0.4070	0.2855	0.2686	0.2502	0.1146	0.3154	0.4167	0.1627	0.2137
551.00	0.000909	7.6399	640.	628.	196.500	1907.	0.4066	0.2855	0.2659	0.2494	0.0916	0.3161	0.4342	0.1437	0.2221
560.00	0.000923	7.4629	624.	589.	629.500	2327.	0.4067	0.3417	0.2998	0.6686	0.3220	0.0	0.2590	0.0	0.1295
561.00	0.000935	7.2606	610.	568.	363.230	2110.	0.4067	0.3237	0.2943	0.4848	0.2147	0.1375	0.3104	0.0643	0.1563
562.00	0.000942	7.1130	602.	583.	270.100	2045.	0.4059	0.3151	0.2923	0.4143	0.2214	0.1855	0.3352	0.0944	0.1564
563.00	0.000947	7.0640	596.	581.	210.000	1998.	0.4059	0.3017	0.2824	0.3468	0.1860	0.2400	0.3587	0.1217	0.1813
564.00	0.000954	7.090Y	588.	578.	131.100	1914.	0.4059	0.2855	0.2721	0.2362	0.1268	0.3214	0.4031	0.1638	0.2048
565.00	0.000954	6.8468	568.	579.	131.900	2004.	0.4321	0.1708	0.1509	0.3028	0.2014	0.3542	0.4340	0.1803	0.2204
566.00	0.000950	7.1900	593.	579.	215.200	1987.	0.4321	0.1980	0.1654	0.3599	0.1964	0.3248	0.4556	0.1274	0.1994
567.00	0.000945	6.9837	598.	580.	277.800	2183.	0.4321	0.2143	0.1800	0.4990	0.3213	0.1941	0.3372	0.0938	0.1684
568.00	0.000943	7.0545	601.	580.	346.030	2269.	0.4321	0.2258	0.1860	0.5672	0.3622	0.1456	0.3266	0.0717	0.1521
569.00	0.000929	7.3290	617.	583.	618.700	2508.	0.4321	0.260C	0.2027	0.7482	0.4515	0.0	0.2351	0.0	0.1175
570.00	0.001009	6.0686	531.	520.	201.900	2632.	0.4311	0.2623	0.2436	0.7514	0.6561	0.0	0.0717	0.0	0.0269
571.00	0.001013	5.6610	527.	52C.	122.000	2317.	0.4311	0.2226	0.2078	0.5567	0.4820	0.1567	0.2142	0.0776	0.1063
572.00	0.001014	5.6642	526.	519.	68.950	2301.	0.4311	0.2011	0.1887	0.5043	0.4459	0.2052	0.2479	0.1031	0.1244
573.00	0.001021	5.7880	519.	520.	80.190	2139.	0.4311	0.1924	0.1807	0.4516	0.3571	0.2842	0.3136	0.1367	0.1589
574.00	0.001016	6.3864	524.	520.	107.300	2037.	0.4311	0.1755	0.1584	0.3404	0.2555	0.3308	0.3965	0.1570	0.1999
575.00	0.001016	5.7722	524.	520.	46.150	1978.	0.4311	0.1604	0.1523	0.2654	0.2263	0.3895	0.4196	0.1944	0.2131
576.00	0.001013	5.9192	527.	520.	62.320	2026.	0.4082	0.2828	0.2755	0.2692	0.2179	0.3063	0.3430	0.1554	0.1738
577.00	0.001012	5.7083	528.	520.	73.800	2133.	0.4082	0.3000	0.2923	0.3700	0.3153	0.2288	0.2581	0.1145	0.1345
578.00	0.001011	5.7293	529.	520.	90.350	2211.	0.4082	0.3089	0.3033	0.4350	0.3728	0.1806	0.2255	0.0892	0.1115
579.00	0.001005	5.9664	529.	521.	144.500	2352.	0.4082	0.3223	0.3106	0.5442	0.4566	0.0993	0.1634	0.0474	0.0798
580.00	0.001010	5.8392	530.	520.	151.030	2501.	0.4082	0.3306	0.3195	0.6270	0.5453	0.0186	0.0943	0.0175	0.0473
581.00	0.001005	5.5403	531.	52C.	184.600	2620.	0.4558	0.3377	0.3253	0.6760	0.5827	0.0	0.0675	0.0	0.0337
590.00	0.001117	4.5419	435.	0.	49.620	3067.	0.4267	0.1954	0.1889	0.8115	0.7860	0.0	0.3167	0.0	0.0084
591.00	0.001070	5.1849	475.	470.	43.130	3047.	0.4267	0.1954	0.1847	0.8115	0.7696	0.0	0.0304	0.0	0.0152

TABLE II

TABLE III

TABLE IV - Selection of Experimental Data

Selection of runs for activation energy determination
(Table II, Figures 7 and 8)

<u>Reason</u>

Planned:	Runs 519 - 551	
Dropped:	Run 519	Reaction rate so low that analyses were in doubt
Used:	Runs 520 - 551	

Selection of runs for rate constant determination
(Table III)

Planned:	Runs 560 - 581	
Dropped:	Runs 560 - 569 (entire 580° bath temperature series)	High difference between wall and reactor temperatures due to generally high conversions caused doubt as to actual reaction temperature.
Added:	Runs 519 - 528.1 538.5 - 546.1	Lower temperature runs from activation energy series replaced above data.
Used:	Runs 519 - 528.1 538.5-546.1 570 - 581	

Runs 590 and 591 were extra runs not planned and not used.

23

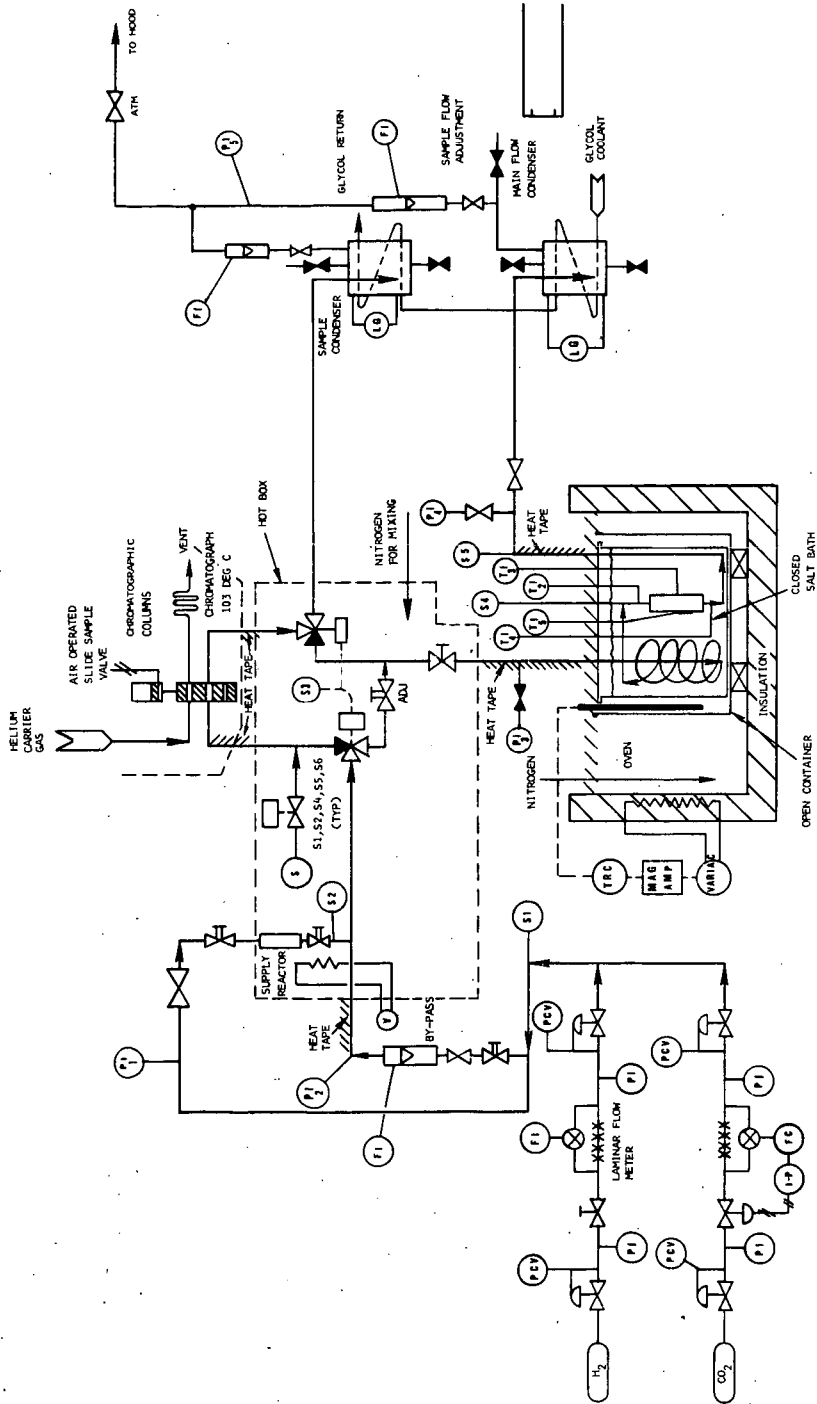FIGURE 1 THERMODYNAMIC EQUILIBRIA FOR THE SABATIER REACTION
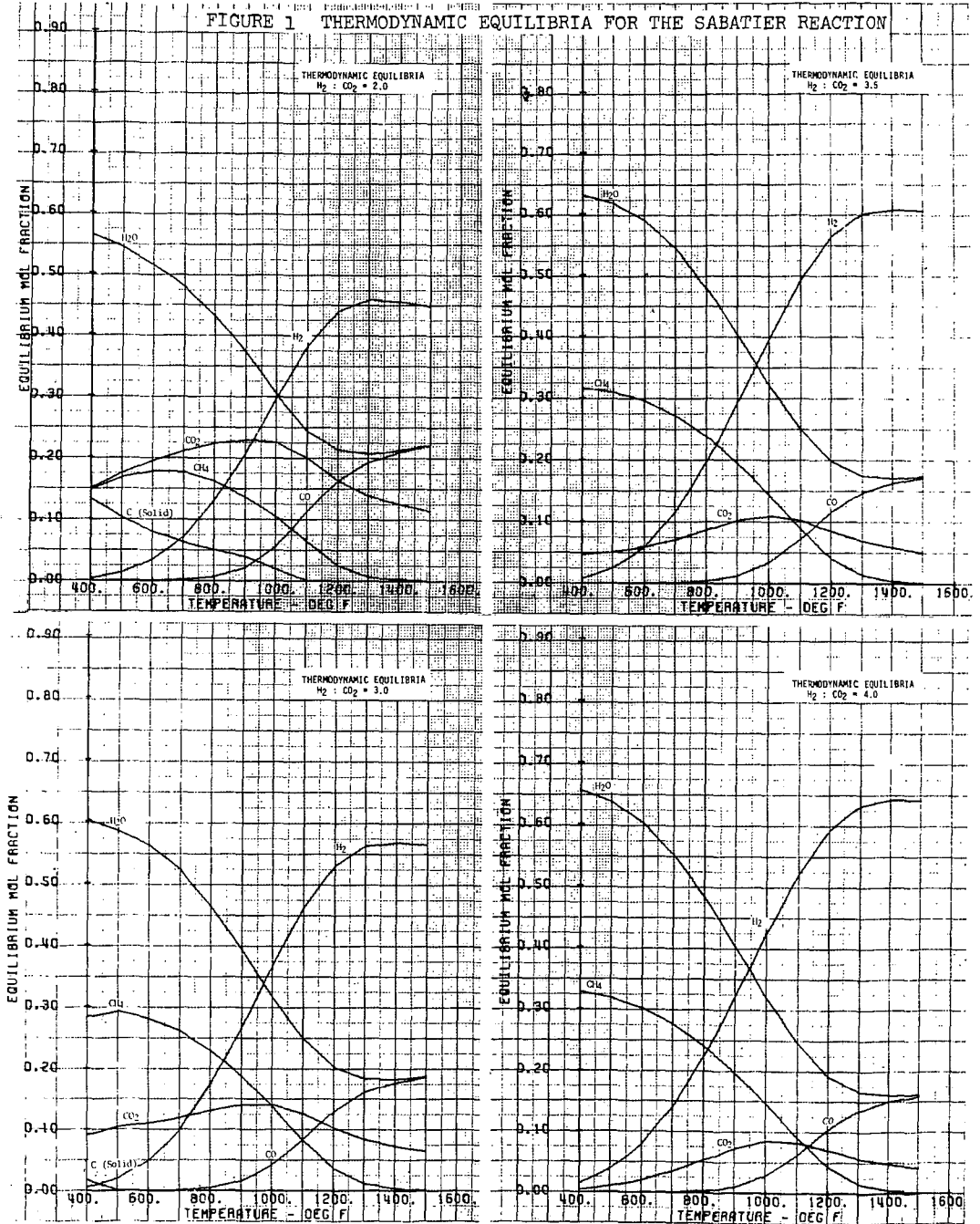
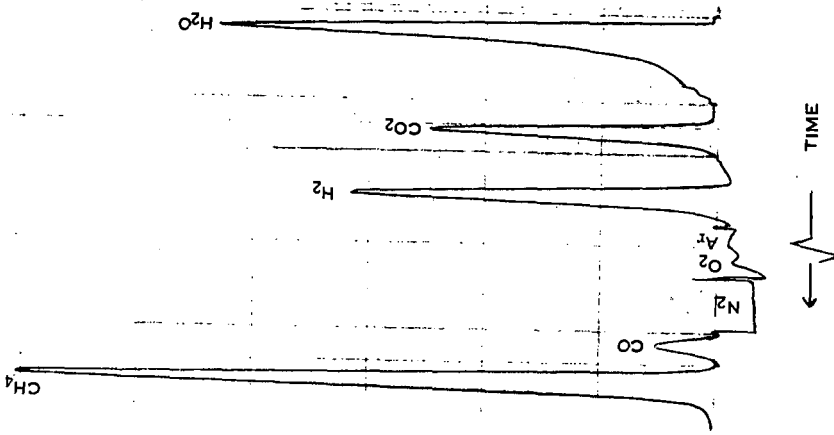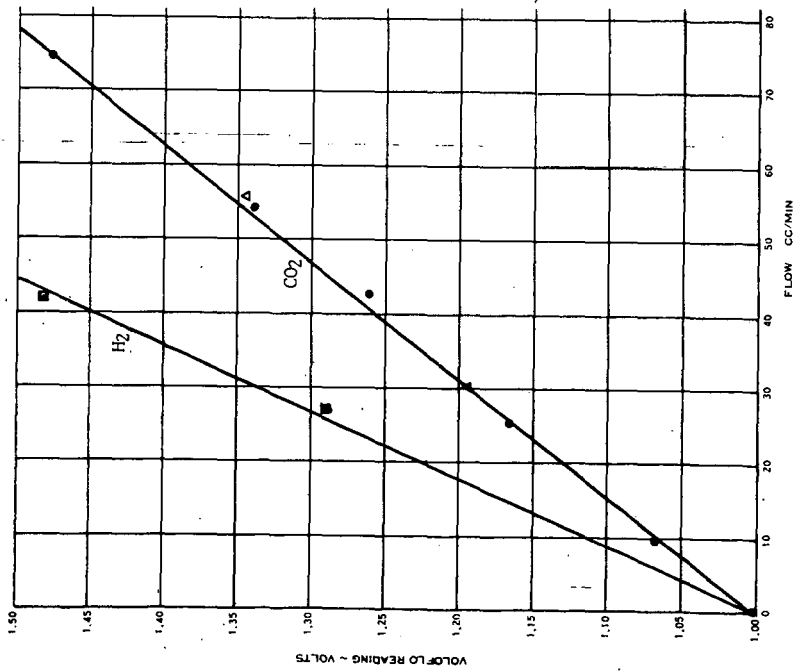FIGURE 2.   RATE DATA APPARATUS, SABATIER REACTION

FIGURE 4   CHROMATOGRAPHIC TRACE
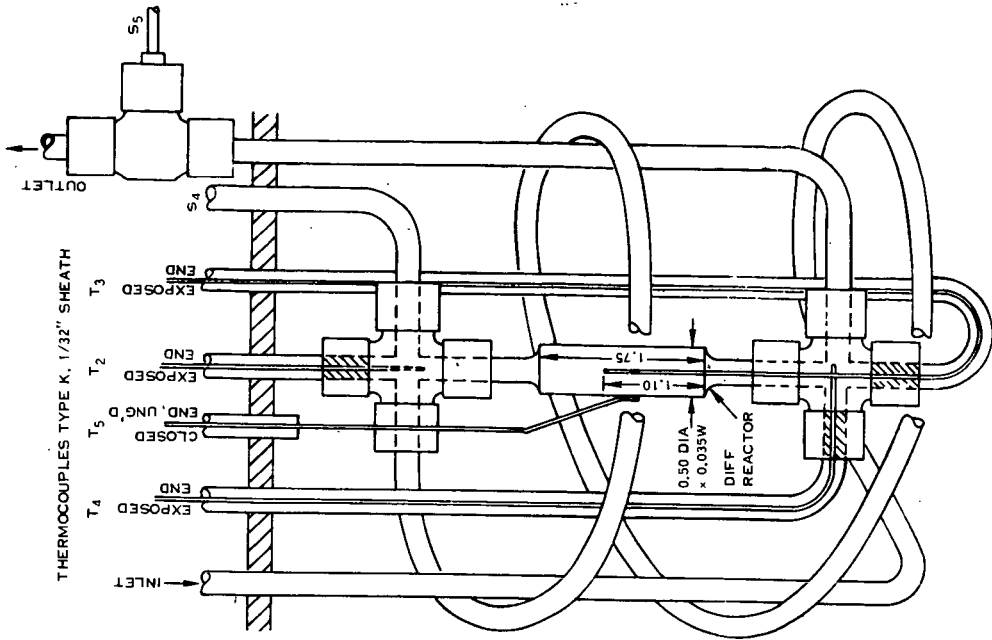

FIGURE 3   VOLOFLO CALIBRATION CURVE FOR CO_2 AND H_2

THERMOCOUPLES TYPE K, 1/32" SHEATH

FIGURE 6 TEST REACTOR SABATIER

CHROMATOGRAPH CALIBRATIONS

FIGURE 5

PEAK HEIGHT, INCHES

PARTIAL PRESSURE, ATM.

FIGURE 8. ACTIVATION ENERGY PLOT

$E_a = 35,700$ BTU/LB–MOL CO_2

$$Y = \ln \frac{Rn}{\left[P_{CO_2}^{3/8} P_{H_2}^{3/2} - \frac{1}{K_{Eq}^{3/8}} P_{CH_4}^{3/8} P_{H_2O}^{3/4} \right]}$$

$1/T \times 10^4$ ($°R^{-1}$)

FIGURE 7. ACTIVATION ENERGY PLOT

$E_a = 30,593$ BTU/LB. MOL CO_2

$$Y = \ln \frac{Rn}{\left[P_{CO_2}^{1/4} P_{H_2} - \frac{1}{K_{Eq}^{1/4}} P_{CH_4}^{1/4} P_{H_2O}^{1/2} \right]}$$

$1/T \times 10^4$ ($°R^{-1}$)